JOURNAL OF BACTERIOLOGY, Apr. 2008, p. 2911–2919 Vol. 190, No. 8
0021-9193/08/$08.00+0 doi:10.1128/JB.01486-07

Binding of the Major Phasin, PhaP1, from *Ralstonia eutropha* H16 to Poly(3-Hydroxybutyrate) Granules▽

Liv Neumann,[1] Francesco Spinozzi,[2] Raffaele Sinibaldi,[2] Franco Rustichelli,[2] Markus Pötter,[1] and Alexander Steinbüchel[1]*

Institut für Molekulare Mikrobiologie und Biotechnologie, Westfälische Wilhelms-Universität, D-48149 Münster, Germany,[1] *and Dipartimento di Scienze Applicate ai Sistemi Complessi (SASC), Sezione di Scienze Fisiche, Università Politecnica delle Marche, Via Ranieri 6, 60131 Ancona, Italy*[2]

Received 14 September 2007/Accepted 11 January 2008

The surface of polyhydroxybutyrate (PHB) storage granules in bacteria is covered mainly by proteins referred to as phasins. The layer of phasins stabilizes the granules and prevents coalescence of separated granules in the cytoplasm and nonspecific binding of other proteins to the hydrophobic surfaces of the granules. Phasin PhaP1$_{Reu}$ is the major surface protein of PHB granules in *Ralstonia eutropha* H16 and occurs along with three homologues (PhaP2, PhaP3, and PhaP4) that have the capacity to bind to PHB granules but are present at minor levels. All four phasins lack a highly conserved domain but share homologous hydrophobic regions. To identify the region of PhaP1$_{Reu}$ which is responsible for the binding of the protein to the granules, N-terminal and C-terminal fusions of enhanced green fluorescent protein with PhaP1$_{Reu}$ or various regions of PhaP1$_{Reu}$ were generated by recombinant techniques. The fusions were localized in the cells of various recombinant strains by fluorescence microscopy, and their presence in different subcellular protein fractions was determined by immunodetection of blotted proteins. The fusions were also analyzed to determine their capacities to bind to isolated PHB granules in vitro. The results of these studies indicated that unlike the phasin of *Rhodococcus ruber*, there is no discrete binding motif; instead, several regions of PhaP1$_{Reu}$ contribute to the binding of this protein to the surface of the granules. The conclusions are supported by the results of a small-angle X-ray scattering analysis of purified PhaP1$_{Reu}$, which revealed that PhaP1$_{Reu}$ is a planar, triangular protein that occurs as trimer. This study provides new insights into the structure of the PHB granule surface, and the results should also have an impact on potential biotechnological applications of phasin fusion proteins and PHB granules in nanobiotechnology.

Many biopolymers are important reserve compounds that are stored in the cytoplasm as insoluble inclusions (14). The best-studied storage compounds in bacteria are polyhydroxyalkanoates (PHAs), and poly(3-hydroxybutyrate) (PHB) is the most prominent example. In most bacteria accumulation of PHAs occurs if an excess amount of a carbon source is present and if growth is concomitantly limited by the lack of another essential nutrient, like nitrogen, phosphorus, oxygen, or something else (45, 49). Therefore, PHAs serve as storage compounds for energy and carbon under starvation conditions. PHA synthesis results in the formation of multiple cytoplasmic inclusions that are generally 200 to 500 nm in diameter in the final accumulation phase (1). The first investigations of PHB granules in bacteria were performed by Williamson and Wilkinson (57) and by Griebel et al. (8). Isolated PHB granules contain approximately 97.5% PHA, 2% protein, and 0.5% phospholipids (8), although some estimates of the lipid contents have been considerably higher (50).

Phasins are small amphiphilic proteins which are localized at the surface of PHB granules and are synthesized by PHB-accumulating bacterium under conditions permissive for PHB synthesis (41, 42). The gram-negative bacterium *Ralstonia eutropha* is used as a model organism to study all aspects of PHB metabolism and has four different phasin proteins (39, 36). PhaP1$_{Reu}$ is the major phasin, and the cells produce large amounts of this protein. Expression of PhaP1$_{Reu}$ is strictly regulated by PhaR$_{Reu}$ at the transcription level (38). The phasins sensu stricto, which includes PhaP1$_{Reu}$, stabilize the dispersion of the hydrophobic PHB granules in the cytoplasm on the one hand and prevent the nonspecific binding of other proteins to the surface of the PHB granules on the other hand. The cells of PhaP1$_{Reu}$-negative mutants of *R. eutropha* have only a single large PHB granule, whereas the wild type has several medium-size granules (56). It was previously shown that lysozyme of *Gallus gallus* binds to PHB granules during isolation of the granules from cells of *Allochromatium vinosum* (23). It was also shown that the β-lactamase (24) and heat shock protein HspA (51) bind to PHB granules in recombinant strains of *Escherichia coli* accumulating PHB. Binding of the latter protein is suppressed in *E. coli* if the PHB biosynthesis enzymes are coexpressed together with PhaP1$_{Reu}$. Besides PhaP1$_{Reu}$, minor amounts of three additional phasin proteins (PhaP2$_{Reu}$, PhaP3$_{Reu}$, and PhaP4$_{Reu}$) occur in *R. eutropha*. Due to the small amounts, it is unlikely that these minor phasins have the same functions as PhaP1$_{Reu}$; however, their physiological or structural functions are not known yet.

Therefore, phasins sensu stricto are interesting structural proteins with unique properties and possibly structures. Since they may also be used for various biotechnological applications, it is necessary to understand the binding of the phasins to

* Corresponding author. Mailing address: Institut für Molekulare Mikrobiologie und Biotechnologie, Westfälische Wilhelms-Universität Münster, Corrensstraße 3, D-48149 Münster, Germany. Phone: 49-251-833 9821. Fax: 49-251-833 8388. E-mail: steinbu@uni-muenster.de.

▽ Published ahead of print on 25 January 2008.

TABLE 1. Bacteria and plasmids used in this study

Strain or plasmid	Description	Source or reference
Strains		
E. coli Top10	F$^-$ *mcrA* Δ(*mrr-hsdRMS-mcrBC*) ϕ80 *lacZ*Δ*M15* Δ*lacX74 deoR recA1 araD139* Δ(*ara-leu*)*7697 galU galK rpsL endA1 nupG*	Invitrogen
E. coli S17-1	*thi proA hsdR17 hsdM*$^+$ *recA* RP4-*tra* function	47
R. eutropha H16	Wild type	DSM 428[a]
R. eutropha Δ*phaP1*	*phaP1* precise deletion gene replacement strain (Re1052), derived from *R. eutropha* H16	58
Plasmids		
pEGFP-N3	Km^r Neo^r *egfp*, pMB1 ori	BD Biosciences
pBBR1MCS-2	Broad-host-range, Km^r *lacPOZ mobRP4*	19
pJAM2::*phaP1-egfp*	pJAM2 harboring *phaP1-egfp* fusion	12
pBBR1MCS-2::*phaP1*$_{Reu}$	pBBR1MCS-2 harboring PCR product comprising *phaP1*	This study
pBBR1MCS-2::*egfp*	pBBR1MCS-2 harboring PCR product comprising *egfp*	This study
pBBR1MCS-2::*phaP1*$_{Reu}$*-egfp*	pBBR1MCS-2 harboring PCR product comprising *phaP1*$_{Reu}$*-egfp*	This study
pBBR1MCS-2::*egfp-phaP1*$_{Reu}$	pBBR1MCS-2 harboring PCR product comprising *egfp-phaP1*$_{Reu}$	This study
pBBR1MCS-2::*phaP1*$_{Reu}$[52>C]*-egfp*	pBBR1MCS-2 harboring PCR product comprising *phaP1*$_{Reu}$[52>C]*-egfp*	This study
pBBR1MCS-2::*phaP1*$_{Reu}$[113>C]*-egfp*	pBBR1MCS-2 harboring PCR product comprising *phaP1*$_{Reu}$[113>C]*-egfp*	This study
pBBR1MCS-2::*phaP1*$_{Reu}$[ΔM]*-egfp*	pBBR1MCS-2 harboring PCR product comprising *phaP1*$_{Reu}$[ΔM]*-egfp*	This study
pBBR1MCS-2::*phaP1*$_{Reu}$[52-112]*-egfp*	pBBR1MCS-2 harboring PCR product comprising *phaP1*$_{Reu}$[52-112]*-egfp*	This study
pBBR1MCS-2::*phaP1*$_{Reu}$[1-85]*-egfp*	pBBR1MCS-2 harboring PCR product comprising *phaP1*$_{Reu}$[1-85]*-egfp*	This study
pBBR1MCS-2::*egfp-phaP1*$_{Reu}$[N>85]	pBBR1MCS-2 harboring PCR product comprising *egfp-phaP1*$_{Reu}$[N>85]	This study
pBBR1MCS-2::*egfp-phaP1*$_{Reu}$[N>112]	pBBR1MCS-2 harboring PCR product comprising *egfp-phaP1*$_{Reu}$[N>112]	This study
pBBR1MCS-2::*egfp-phaP1*$_{Reu}$[ΔM]	pBBR1MCS-2 harboring PCR product comprising *egfp-phaP1*$_{Reu}$[ΔM]	This study
pBBR1MCS-2::*egfp-phaP1*$_{Reu}$[52-112]	pBBR1MCS-2 harboring PCR product comprising *egfp-phaP1*$_{Reu}$[52-112]	This study

[a] DSM, Deutsche Sammlung für Mikroorganismen und Zellkulturen.

PHB granules. In the 14-kDa phasin of the gram-positive organism *Rhodococcus ruber* (34) two short stretches comprising about 8 hydrophobic amino acids were identified close to the C-terminal region. If one or both stretches were removed from this protein, the truncated phasin was no longer capable of binding to the granules and occurred in the cytoplasm (35). If, on the other hand, the short region of this phasin comprising the two hydrophobic stretches was fused with an acetaldehyde dehydrogenase of *R. eutropha*, the fusion protein bound in vivo as well as in vitro to PHB granules (35). This was the first demonstration that phasins can be used as anchors for binding of other proteins to the surface of PHB granules. This was later confirmed and also demonstrated for other fusion proteins with PhaP1$_{Reu}$ (3, 2) and also with the PHA granule-associated protein PhaF$_{Ppu}$ of *Pseudomonas putida* (26) in other laboratories. Furthermore, it was recently shown that other proteins involved in PHA metabolism, like a fusion of the substrate-binding domain of a PHA depolymerase (22, 30) or of PHA synthases (32, 33), can be used to immobilize other proteins with PHA. Similarly, PhaP1$_{Reu}$ fused to other proteins also binds intracellularly to triacylglycerol inclusions in oleogenous actinomycetes (12) like eukaryotic lipid body proteins bind to these hydrophobic inclusions (13).

The aims of this study were to identify the region in PhaP1$_{Reu}$ of *R. eutropha* which mediates binding of this phasin to PHB granules and to obtain some information about the structure of PhaP1, thereby also contributing to our understanding of phasins.

MATERIALS AND METHODS

Bacterial strains and plasmids. The bacterial strains and plasmids used in this study are shown in Table 1.

Media and cultivation of cells. Cells of *R. eutropha* were grown at 30°C in mineral salts medium supplemented with 1.0% (wt/vol) sodium gluconate (46). Solid media contained 1.5% (wt/vol) purified agar. Cells of *E. coli* were cultivated at 37°C in Luria-Bertani medium (44).

Isolation of PHB granules. For isolation of PHB granules a modification of the method of Wieczorek et al. (56) was used. Cells of an *R. eutropha* Δ*phaP1* mutant were grown in mineral salts medium under storage conditions. The cells were cultivated for 72 h, harvested by centrifugation (20 min, 6,000 × *g*, 4°C), washed and resuspended in Tris-HCl buffer (10 mM, pH 7.0), and disrupted by a three passages through a French press (100 × 10^6 Pa). The disrupted cells were layered on top of a discontinuous glycerol gradient consisting of 5 ml of (vol/vol) glycerol 90% and 5 ml of 60% (vol/vol) glycerol. After ultracentrifugation (60 min, 100,000 × *g*, 4°C) the PHB granules formed a layer between the two phases and could be separated. The isolated granules were washed three times with Tris-HCl buffer (10 mM, pH 7.0) and stored at −20°C.

Purification of PhaP1$_{Reu}$. PhaP1$_{Reu}$ was purified from PHB granules isolated from *R. eutropha* cells by detergent treatment as described previously (56).

Polyacrylamide gel electrophoresis and Western immunoblotting. Protein samples were resuspended in gel loading buffer (0.6% [wt/vol] sodium dodecyl sulfate [SDS], 1.25% [wt/vol] β-mercaptoethanol, 0.25 mM EDTA, 10% [vol/vol] glycerol, 0.001% [wt/vol] bromophenol blue, 12.5 mM Tris-HCl; pH 6.8) and separated in 12.5% (wt/vol) SDS-polyacrylamide gels, as described by Laemmli (21). Proteins were stained with Coomassie brilliant blue R-250 (54). Immunological detection of enhanced green fluorescent protein (EGFP) fusion proteins blotted from the SDS-polyacrylamide gel onto polyvinylidene difluoride-nitrocellulose membranes was performed exactly as described by Towbin et al. (53), using polyclonal EGFP antibodies (BD Biosciences).

Molecular weight determination by gel filtration. A Superdex 200 HP column (XK 26/60; GE Healthcare) was equilibrated with 50 ml of 100 mM potassium phosphate buffer (pH 7.0). Purified protein and calibration proteins (1.0 mg each) were applied to the column and eluted at a flow rate of 0.5 ml/min.

TABLE 2. Oligonucleotides used for PCR amplification and other purposes in this study

Oligonucleotide	Sequence	Location and orientation
PhaP1_N_XhoI	5′-AAA CTC GAG AAG GAG GGA TCC ATG ATC CTC ACC CCG G-3′	5′ region of *phaP1*$_{Reu}$
EGFP_C_HindIII	5′-AAA AAG CTT TTA CTT GTA CAG CTC GTC CAT GCC-3′	3′ region of *egfp*
EGFP_C_EcoRI	5′-G GCC GAA TTC CTT GTA CAG CTC GTC CAT GCC G-3′	5′ region of *egfp*
EGFP_N_MCS(SalI)	5′-T TCT GCA GTC GAC GGT ACC GC-3′	3′ region of *egfp*
PhaP(Re)_C_HindIII	5′-GC AGA AGC TTA TCA GGC AGC CGT CGT CTT C-3′	3′ region of *phaP1*$_{Reu}$
PhaP(Re)_N_EcoRI	5′-G AGA GAA TTC ATG ATC CTC ACC CCG GAA CAA G-3′	5′ region of *phaP1*$_{Reu}$
PhaP-52C	5′-A GAA CTC GAG GAG AAG GCC ATG AAG GCG CTG TCG GCC AAG-3′	5′ region of truncated *phaP1*$_{Reu}$
PhaP-N85-rev	5′-GA AAA GCT TTC TTA CAG GTG GCG GGT GTA GGC-3′	3′ region of truncated *phaP1*$_{Reu}$
PhaP-113C	5′-C GAA CTC GAG AAG AAC GTG CAA ATG CTG GTC GAG AAC CTC GCC-3′	5′ region of truncated *phaP1*$_{Reu}$
PhaP-N112-rev	5′-AC CAA AGC TTA CAC GTT CTT CGA GCC TTC GG-3′	3′ region of truncated *phaP1*$_{Reu}$
P-EGFP-EcoRI-N	5′-G AGG GAA TTC ATG GTG AGC AAG GGC GAG GAG C-3′	5′ region of *egfp*
PhaP(112)_EcoRI_C	5′-A AAA GAA TTC CAC GTT CTT CGA GCC TTC GG-3′	3′ region of *egfp*
PhaP(52C)_EcoRI_N	5′-A AAA GAA TTC AAG GCG CTG TCG GCC AAG-3′	3′ region of truncated *phaP1*$_{Reu}$
PhaP1–85_C_EcoRI	5′-C CGA GAA TTC GCC GCC GCC GTG GCG GGT GTA GGC CAG G-3′	3′ region of truncated *phaP1*$_{Reu}$

Relative molecular masses were calculated from semilogarithmic plots of the molecular masses of calibration proteins versus elution volume.

Isolation, amplification, and manipulation of DNA. Chromosomal DNA of *R. eutropha* H16 was isolated by the method of Marmur (25). Plasmid DNA was isolated by the method of Birnboim and Doly (5). DNA restriction fragments were purified with a Perfectprep gel cleanup kit, as described by the manufacturer (Eppendorf). Restriction enzymes, ligases, and other enzymes used for DNA manipulation were used according to the manufacturers' instructions.

All PCR amplifications were carried out as described by Sambrook et al. (44), employing *Pfx* DNA polymerase (Invitrogen) and an Omnigene HBTR3CM DNA thermal cycler (Hybaid). All oligonucleotides which were used as primers for PCR amplification or other purposes are shown in Table 2.

Construction of hybrid plasmids encoding fusions of the *egfp* gene with the *phaP1* gene or parts of the *phaP1* gene. The *phaP1*$_{Reu}$*-egfp* fusion fragment was amplified by PCR using plasmid pJAM2::*phaP1-egfp* (12) as the template and oligonucleotides PhaP1_N_XhoI and EGFP_C_HindIII (Table 2) as the primers. The resulting PCR product (1.3 kbp) was restricted with XhoI and HindIII and cloned into vector pBBR1MCS-2, which was treated with the same restriction endonucleases, yielding hybrid plasmid pBBR1MCS-2::*phaP1*$_{Reu}$*-egfp*. The *egfp-phaP1*$_{Reu}$ fusion was obtained by amplification of both fragments. The *egfp*-fragment (0.8 kbp) was amplified from plasmid pEGFP-N3 by performing PCR using oligonucleotides EGFP_N_MCS(SalI) and EGFP_C_EcoRI. The *phaP1*$_{Reu}$ fragment (0.6 kbp) was amplified with oligonucleotides PhaP(Re)_N_EcoRI and PhaP(Re)_C_HindIII from genomic DNA of *R. eutropha* H16. The PCR products obtained were then digested with EcoRI and ligated. The ligation product was then amplified by PCR using oligonucleotides EGFP_N_MCS(SalI) and PhaP(Re)_C_HindIII. The resulting fusion product (1.4 kbp) was restricted with SalI and HindIII and cloned into the vector pBBR1MCS-2, yielding hybrid plasmid pBBR1MCS-2::*egfp-phaP1*$_{Reu}$.

For control experiments the genes encoding EGFP and PhaP1$_{Reu}$ were cloned using the same vector, which yielded plasmids pBBR1MCS-2::*egfp* and pBBR1MCS-2::*phaP1*$_{Reu}$. The *phaP1*$_{Reu}$ gene was amplified from genomic DNA of *R. eutropha* H16 using oligonucleotides PhaP1_N_XhoI and PhaP1(Re)_C_HindIII (Table 2). The resulting fragment (0.6 kbp) was digested with XhoI und HindIII and cloned into plasmid pBBR1MCS-2, which was restricted with the same enzymes. The *egfp* fragment was obtained by performing PCR with pEGFP-N3 as the template and oligonucleotides EGFP_N_MCS(SalI) and EGFP_C_HindIII. The PCR product (0.8 kbp) was restricted with SalI and HindIII and ligated to SalI- and HindIII-digested pBBR1MCS-2 DNA, yielding pBBR1MCS-2::*egfp*.

Truncated versions of PhaP1$_{Reu}$ fused to EGFP (PhaP1$_{Reu}$[52>C]-EGFP, PhaP1$_{Reu}$[113>C]-EGFP, EGFP-PhaP1$_{Reu}$[N>112], EGFP-PhaP1$_{Reu}$[N>85]) were prepared by performing PCR using different primer combinations (Table 2) and plasmids pBBR1MCS-2::*egfp-phaP1*$_{Reu}$ and pBBR1MCS-2::*phaP1*$_{Reu}$*-egfp* PCR as the templates. Hybrid plasmids pBBR1MCS-2::*phaP1*$_{Reu}$[ΔM]*-egfp* and pBBR1MCS-2::*egfp-phaP1*$_{Reu}$[ΔM] were constructed by digestion of the PCR products (*phaP1*$_{Reu}$*-egfp* and *egfp-phaP1*$_{Reu}$) with MscI, which deleted the nucleotides coding for amino acids 65 to 131 in frame. Hybrid plasmids pBBR1MCS-2::*phaP1*$_{Reu}$[1-85]*-egfp*, pBBR1MCS-2::*phaP1*$_{Reu}$[52-112]*-egfp*, and pBBR1MCS-2::egfp-*phaP1*$_{Reu}$[52-112] were constructed by PCR amplification employing the oligonucleotides shown in Table 2 for both fragments and the fusion product as described above for the *egfp-phaP1*$_{Reu}$ fusion.

DNA sequencing. DNA sequencing was performed by using a SequiTherm EXCEL TM II long read cycle sequencing kit (Epicenter Technologies), IRD800-labeled oligonucleotides (MWG-Biotech), and a Li-Cor 4000L (Li-Cor Biosciences) automated sequencer (MWG-Biotech).

Transfer of DNA. Competent cells of *E. coli* were prepared and transformed by using the $CaCl_2$ procedure described by Hanahan (11). Transfer of DNA to *R. eutropha* strains by conjugation was performed by spot agar mating as described by Friedrich et al. (7) using *E. coli* S17-1 harboring the desired plasmid as the donor.

Theory of SAXS analyses. The small-angle X-ray scattering technique (SAXS) is a powerful tool able to detect the shape and conformational and aggregational states of proteins in solution for a broad range of conditions and sizes. In a SAXS experiment, a protein solution is exposed to a focused X-ray beam, and the scattered intensity is collected as a function of the scattering angle. The theoretical background, basic equations, and methods used for SAXS data analysis have been fully described previously (10, 15, 16, 18, 28, 31, 37, 48, 54).

SAXS analyses. SAXS experiments were performed using a conventional laboratory X-ray Kratky camera. The wavelength of the X-rays was 1.54 Å, and the sample-to-detector distance was 1.5 m. The scattering vector range was 0.022 to 0.2 $Å^{-1}$. A PhaP1$_{Reu}$ sample at a concentration of 6 mg/ml in 10 mM Tris-HCl buffer (pH 7.0) was analyzed using 1.5-mm glass capillaries. The experimental intensity was corrected for background, buffer contribution, detector inhomogeneities, and sample transmission.

Secondary structure predictions for proteins. For PhaP1$_{Reu}$, phasin homologues, and the substrate-binding domain of the *Pseudomonas stutzeri* PHB depolymerase, predictions were made as described by Deleage et al. (6; http://npsa-pbil.ibcp.fr). For predictions of the secondary structure of PhaP1$_{Reu}$ the following algorithms were used: MLRC (9), DSC (17), and PHD (43).

Microscopic analysis of cells containing EGFP fusion proteins. For microscopic localization of EGFP and of EGFP fusion proteins, an Olympus BX51 microscope (Olympus Europe) was used. The fluorescence of the EGFP used could be excited at a wavelength of 488 nm and detected at 507 nm (data for plasmid pEGFP-N3 according to the manufacturer [BD Biosciences]) using a U-MNIBA3 filter combination (excitation wavelength, 470 to 495 nm; emission wavelength, 510 to 550 nm).

RESULTS

Comparison of primary structures of phasins and secondary structure predictions. Sequence and hydrophobicity plot analysis of the four PhaP1$_{Reu}$ phasin homologues in *R. eutropha* H16 revealed a high degree of similarity and several highly conserved amino acids in PhaP1$_{Reu}$, PhaP2$_{Reu}$, PhaP3$_{Reu}$, and PhaP4$_{Reu}$ (Fig. 1A). In contrast, comparison of the primary structures of *R. eutropha* PhaP1$_{Reu}$, *P. putida* PhaF$_{Ppu}$, and *R.*

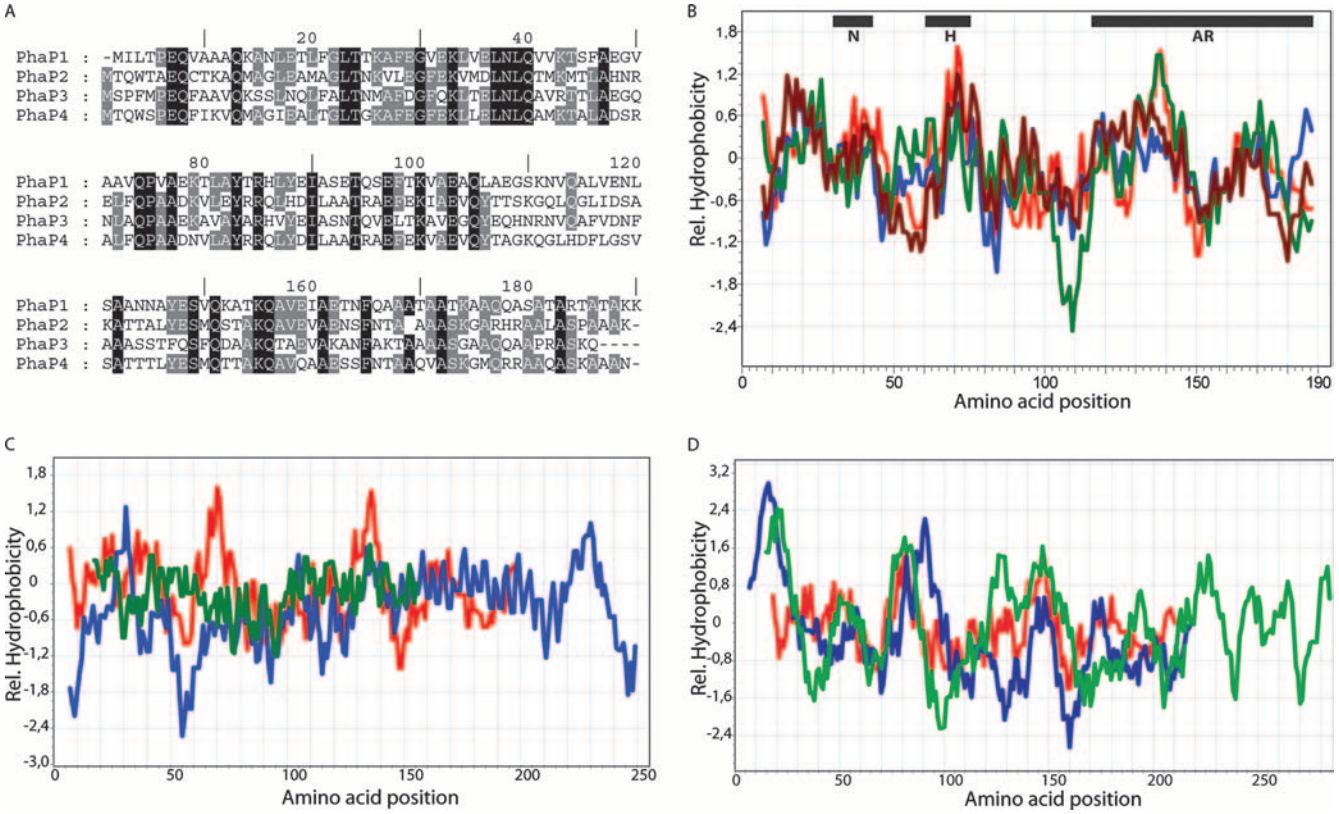

FIG. 1. Primary structure and hydrophobicity of phasins and other proteins that bind to PHB granules. (A) Primary structures of the *R. eutropha* H16 phasins PhaP1$_{Reu}$, PhaP2$_{Reu}$, PhaP3$_{Reu}$, and PhaP4$_{Reu}$. The gray and black backgrounds indicate identities of the amino acids (black background, conserved in all four phasins; gray background, conserved in at least three of the four phasins). (B) Hydrophobicity plot (20) of the four *R. eutropha* H16 phasins. Red line, Phap1$_{Reu}$; blue line, PhaP2$_{Reu}$; green line, PhaP3$_{Reu}$; brown line, PhaP4$_{Reu}$. The regions of interest are an N-terminal conserved part (N), a hydrophobic patch (H), and the alanine-rich C terminus (AR). (C) Hydrophobicity plot (20) of the phasin homologues PhaF$_{Ppu}$ of *P. putida* and GA14$_{Rru}$ of *R. ruber* compared to PhaP1$_{Reu}$. Red line, PhaP1$_{Reu}$; blue line, PhaF$_{Ppu}$; green line, GA14$_{Rru}$. (D) Hydrophobicity plot (20) of the PHB-binding proteins lysozyme (*G. gallus*) and β-lactamase (*E. coli*) compared to PhaP1$_{Reu}$. Red line, PhaP1$_{Reu}$; blue line, lysozyme; green line, β-lactamase. Rel., relative.

ruber GA14$_{Rru}$ revealed only a few highly conserved amino acids in these proteins (data not shown). Therefore, in general, there is not a conserved sequence motif representing a "PHB granule-binding box" in phasins. Binding could be caused by short stretches of hydrophobic proteins, as such stretches were identified in GA14$_{Rru}$ of *R. ruber* (35). Hydrophobicity plots obtained for the four *R. eutropha* phasins (Fig. 1B), for PhaP1$_{Reu}$, PhaF$_{Ppu}$ from *P. putida*, and GA14$_{Rru}$ from *R. ruber* (Fig. 1C), and for PhaP1$_{Reu}$, lysozyme from *G. gallus*, and β-lactamase from *E. coli* (Fig. 1D) did not reveal conserved hydrophobic regions like those that occur, for example, in membrane proteins; in addition, motifs representing minima and maxima occur in different regions of these proteins. PhaF$_{Ppu}$ exhibits a hydrophilic minimum at amino acid positions 50 to 60, and the entire sequence is more hydrophilic than the sequences of PhaP1$_{Reu}$ and GA14$_{Rru}$. GA14$_{Rru}$ is less hydrophobic than PhaP1$_{Reu}$.

The binding of phasins to PHB granules could be caused not only by a discrete motif in the primary structure but also by the secondary, tertiary, or quaternary structure of the protein. Therefore, we performed a secondary structure prediction analysis for various phasins as described by Deleage et al. (6; http://npsa-pbil.ibcp.fr) and in Materials and Methods. We obtained very similar predictions for the phasins sensu stricto, such as the four phasins occurring in *R. eutropha* H16, PhaP1 of *Ralstonia solanacearum*, and *Ralstonia metallidurans*. These phasins share a very high fraction (about 90%) of α-helical structure that could be a characteristic feature of the proteins. Interestingly, the putative PHB-binding domain in the C-terminal region of the regulator PhaR$_{Reu}$ is also α-helical, in contrast to the N-terminal putative DNA-binding domain of this protein (the Pfam version 18.0 domains are PHB_acc_N [amino acids 10 to 73] and PHB_acc [amino acids 75 to 115]) (4; http://www.sanger.ac.uk/Software/Pfam). On the other hand, the substrate-binding domain of the extracellular PHB depolymerase from *P. stutzeri* does not have an analogous α-helical structure. The PHA-binding motif of this protein and that of the *P. putida* phasin PhaF$_{Ppu}$ might be different, as shown by Ohura et al. (29) and Moldes et al. (26).

In vivo binding capacity of EGFP-PhaP1$_{Reu}$ fusion proteins in *E. coli* and *R. eutropha*. Various fusions of *phaP1*$_{Reu}$ and *egfp* were constructed by PCR amplification of different DNA fragments, digestion, ligation, and amplification of the fusion products exactly as described in Materials and Methods.

The capacities of the resulting PhaP1$_{Reu}$-EGFP fusion proteins to bind to PHB granules in cells were then investigated by

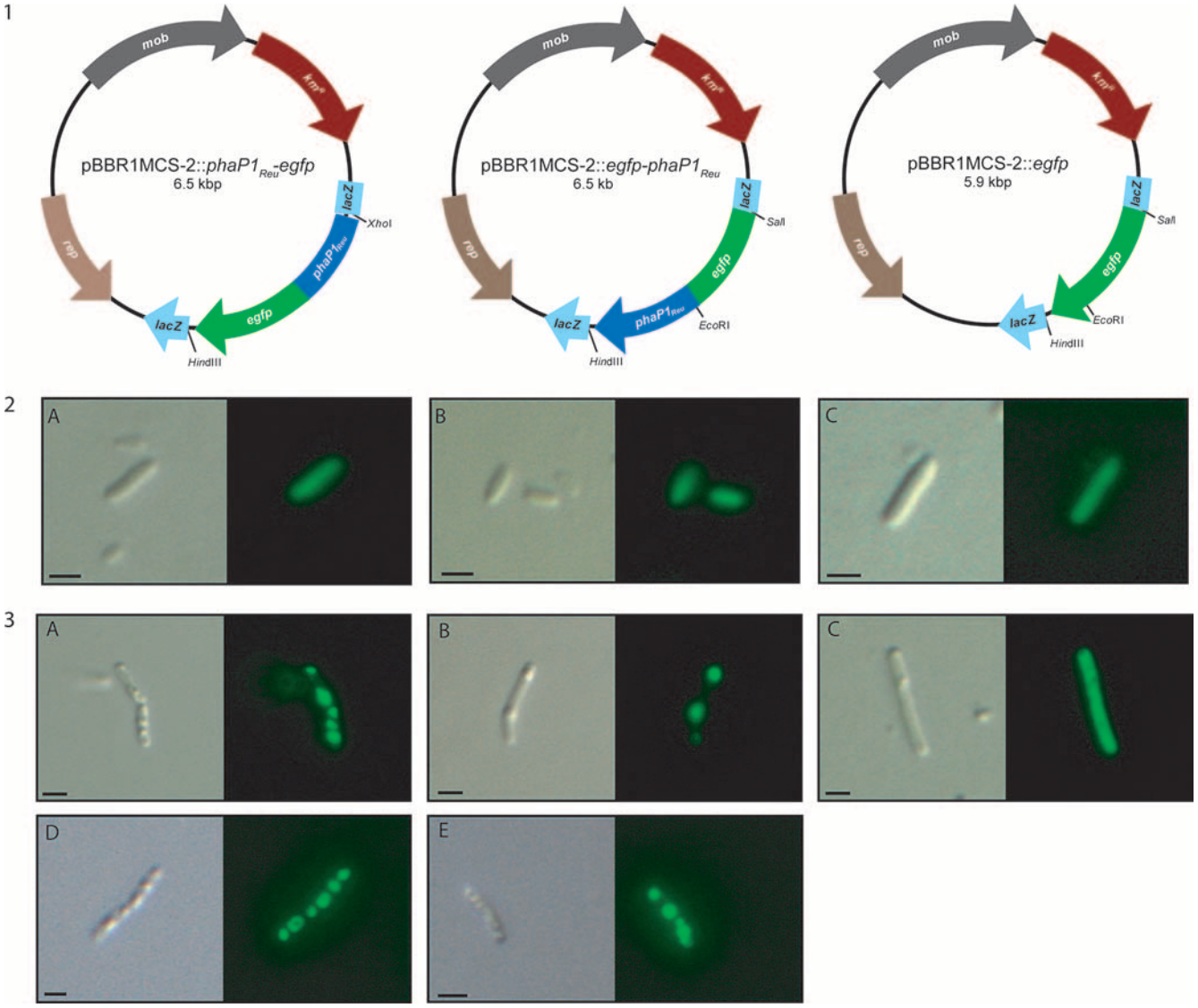

FIG. 2. Distribution of EGFP-PhaP1$_{Reu}$ and PhaP1$_{Reu}$-EFGP fusion proteins in cells of recombinant strains of *E. coli* Top10 and an *R. eutropha* Δ*phap1* mutant. (Panel 1) Plasmids constructed for fluorescence microscopic studies encoding the EGFP-PhaP1$_{Reu}$ and PhaP1$_{Reu}$-EGFP fusion proteins and the EGFP control. *km*^{R}, kanamycin resistance; *lacZ*, α-fragment of the β-galactosidase gene; *mob*, mobilization site; *rep*, origin of replication. (Panel 2) Fluorescence microscopy of *E. coli* Top10 expressing the following fusion proteins: (A) PhaP1$_{Reu}$-EGFP, (B) EGFP-PhaP1$_{Reu}$, and (C) the EGFP control. (Panel 3) Fluorescence microscopy of *R. eutropha* Δ*phap1* mutant (A to C) and *R. eutropha* H16 (D to E) expressing the following fusion proteins: (A) PhaP1$_{Reu}$-EGFP, (B) EGFP-PhaP1$_{Reu}$, (C) EGFP control, (D) PhaP1$_{Reu}$-EGFP, and (E) EGFP-PhaP1$_{Reu}$. Each pair of images consists of a conventional microscopic image (left) and the corresponding fluorescent image (right). The corresponding plasmids are indicated above the images in panel 1. Bars, 1 μm.

fluorescence microscopy. The expression of all proteins could be analyzed in the absence of PHB using cells of *E. coli* harboring the different plasmids (Fig. 2, panel 2). In such cells the fusion proteins showed a diffuse fluorescence that was caused by the homogeneous distribution of the fluorescent proteins inside the entire cytoplasm (Fig. 2, panels 2A and 2B), like cells harboring the EGFP control (Fig. 2, panel 2C). The binding capacities of the fusion proteins were visible in *R. eutropha* Δ*phaP1* and H16 recombinant cells expressing the fusion protein PhaP1$_{Reu}$-EGFP or EGFP-PhaP1$_{Reu}$ (Fig. 2, panels 3A to 3E). In these cells the fluorescence was restricted to the PHB granules.

In vivo binding capacities of truncated PhaP1$_{Reu}$-EGFP fusion proteins in *E. coli* and *R. eutropha*. Various fusions of EGFP to truncated PhaP1$_{Reu}$ proteins lacking either parts of the N-terminal region (PhaP1$_{Reu}$[52>C]-EGFP and PhaP1$_{Reu}$[113>C]-EGFP), parts of the C-terminal region (PhaP1$_{Reu}$[1-85]-EGFP, EGFP-PhaP1$_{Reu}$[N>112], and EGFP-PhaP1$_{Reu}$[N>85]), parts of the N-terminal region plus parts of the C-terminal region (PhaP1$_{Reu}$[52-112]-EGFP and EGFP-PhaP1$_{Reu}$[52-112]), or parts of the central region (PhaP1$_{Reu}$[ΔM]-EGFP and EGFP-PhaP1$_{Reu}$[ΔM]) of the phasin were constructed by PCR as described in Materials and Methods. A schematic overview of all fusion proteins generated in this study is shown in Fig. 3. The

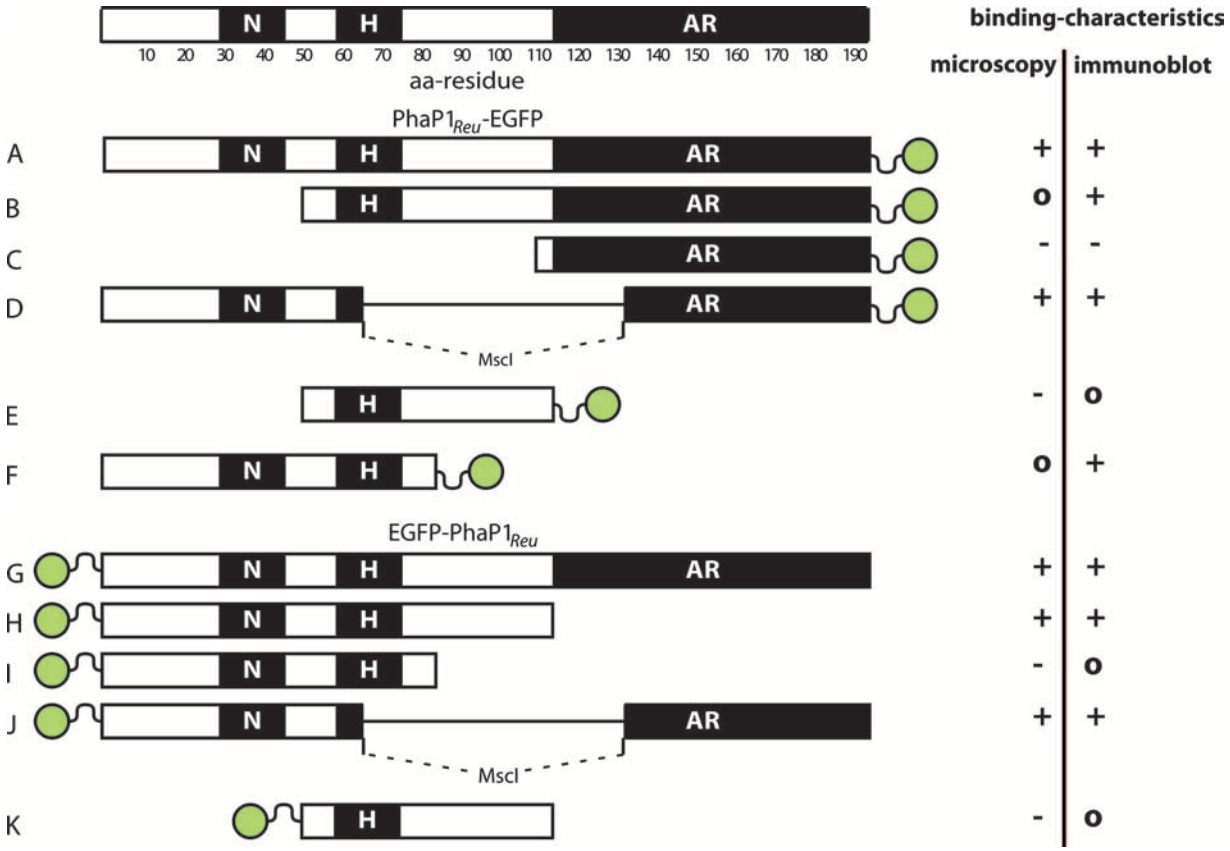

FIG. 3. Summary of EGFP fusions with various regions of PhaP1$_{Reu}$. The position of the EGFP is indicated by a green circle, and the corresponding region of PhaP1$_{Reu}$ used to create the fusion is shown in a schematic diagram. Regions of interest are described in the legend to Fig. 1. Binding characteristics were determined by the microscopic studies and immunoblotting (+, binding; −, no binding; o, unclear). (A) PhaP1$_{Reu}$-EGFP; (B) PhaP1$_{Reu}$[52>C]-EGFP; (C) PhaP1$_{Reu}$[113>C]-EGFP; (D) PhaP1$_{Reu}$[ΔM]-EGFP; (E) PhaP1$_{Reu}$[52-112]-EGFP; (F) PhaP1$_{Reu}$[1-85]-EGFP; (G) EGFP-PhaP1$_{Reu}$; (H) EGFP-PhaP1$_{Reu}$[N>112]; (I) EGFP-PhaP1$_{Reu}$[N>85]; (J) EGFP-PhaP1$_{Reu}$[ΔM]; (K) EGFP-PhaP1$_{Reu}$[52-112]. aa, amino acid.

binding of these fusion proteins to PHB granules was then studied by fluorescence microscopy and compared to the binding of PhaP1$_{Reu}$-EGFP and EGFP-PhaP1$_{Reu}$ to PHB granules. We were especially interested to see whether the binding was mediated by the N-terminal conserved part, the hydrophobic patch, or the alanine-rich C terminus of PhaP1$_{Reu}$ (Fig. 1) and whether one of these regions is responsible for the binding of the whole protein to the PHB granules.

The results of the microscopic analyses of the capacities of truncated fusion proteins to bind to PHB granules are shown in Fig. 4. For the PhaP1$_{Reu}$[ΔM]-EGFP, EGFP-PhaP1$_{Reu}$[N>112], and EGFP-PhaP1$_{Reu}$[ΔM] fusions the fluorescence was restricted to the region containing PHB granules in the cells, thus indicating that the PHB affinities of the PhaP1$_{Reu}$ regions of these fusions were high. In contrast, the PhaP1$_{Reu}$[113>C]-EGFP, PhaP1$_{Reu}$-[52-112]-EGFP, EGFP-PhaP1$_{Reu}$[N>85], and EGFP-PhaP1$_{Reu}$[52-112] fusions showed only diffuse fluorescence, indicating that the regions of PhaP1$_{Reu}$ could obviously not mediate binding of the fusion protein to PHB granules. The other two fusion proteins, PhaP1$_{Reu}$[52>C]-EGFP and PhaP1$_{Reu}$[1-85]-EGFP, gave no clear images.

In summary, the binding of the whole PhaP1$_{Reu}$ protein to PHB granules appears to be greater than the binding of any truncated PhaP1$_{Reu}$, because the fluorescence of the fusions with complete PhaP1 was completely restricted to the granules, whereas truncated fusions always showed higher levels of cytoplasmic fluorescence.

To check the capacity of fusion proteins to bind to PHB granules and to verify the microscopic images for the other proteins, polyacrylamide gel electrophoresis and Western immunoblotting of crude cell extracts and isolated granules were performed (not shown). In the immunoblots of proteins of the crude cell extracts all expressed fusion proteins should have been detectable. In contrast, only PHB-bound fusion proteins should have been present in the immunoblots prepared for isolated granules. The EGFP-PhaP1$_{Reu}$[N>85], EGFP-PhaP1$_{Reu}$[52-112], and PhaP1$_{Reu}$[52-112]-EGFP fusion proteins could not be detected either in crude extracts or in granule fractions. The PhaP1$_{Reu}$[113>C]-EGFP fusion was detected only in the crude extracts and not in the isolated granules. The PhaP1$_{Reu}$[52>C]-EGFP, PhaP1$_{Reu}$[ΔM]-EGFP, PhaP1$_{Reu}$[1-85]-EGFP, EGFP-PhaP1$_{Reu}$[N>112], and EGFP-PhaP1$_{Reu}$[ΔM] fusion proteins were detected in the crude extracts, as well as in the isolated PHB granules. The results of these experiments are summarized in Fig. 3, which provides an overview of the results obtained with all fusion proteins in this study.

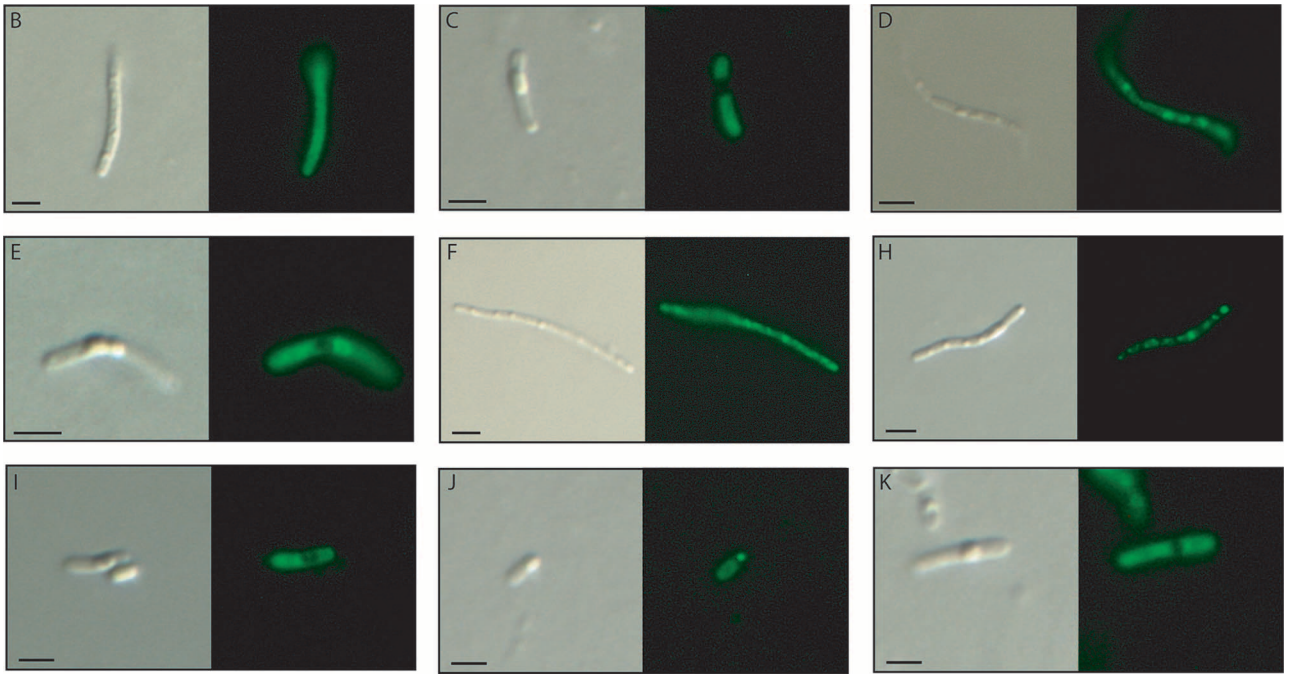

FIG. 4. Distribution of EGFP fusion proteins with various regions of PhaP1$_{Reu}$ in cells of recombinant strains of the *R. eutropha* H16 Δ*phaP1* mutant. Each pair of images consists of a conventional microscopic image (left) and the corresponding fluorescent image (right). The letters correspond to the letters shown on the left in Fig. 3. Bars, 1 μm.

SAXS analysis of purified PhaP1$_{Reu}$. To obtain the first information concerning the quaternary and three-dimensional structure of PhaP1$_{Reu}$, the protein was purified from a recombinant strain of *E. coli* and subjected to SAXS analysis. Experimental SAXS data for PhaP1 are shown in Fig. 5 as a semilogarithmic plot. To assess the particle shape, the SAXS curve was analyzed using the multipole expansion method described in Materials and Methods. The maximum rank was fixed at 4, and the width of the hydration layer at the particle border was fixed at 2 Å. Considering the quality of the data, the final fitting curve, also shown in Fig. 5, seems particularly good. The recovered fitting parameters of the multipole expansion analysis for PhaP1 for an M value of 5 ($a_{l,m}$) are as follows: Re $a_{0,0}$, 10.7 ± 0.1; Re $a_{1,0}$, −0.3 ± 0.1; Re $a_{2,0}$, −1.05 ± 0.03; Re $a_{3,0}$, 0.3 ± 0.1; and Re $a_{3,3}$, 0.10 ± 0.05. It should be noted that the point group symmetry obtained is C_3, with a threefold symmetry axis. The corresponding blunt-end triangular shape function is shown in Fig. 6, which suggests a trimeric aggregation number. The side length of the triangles and the height were calculated to be 80 ± 3 and 26 ± 1 Å, respectively. Further evidence for the hypothesis that PhaP1$_{Reu}$ occurs as a homotrimer was obtained by gel filtration of the purified PhaP1, which revealed a molecular mass of 60 ± 5 kDa for purified PhaP1$_{Reu}$ (data not shown). Further confirmation was obtained from the protein volume, 1.07 × 10^5 ± 0.05 × 10^5 Å^3; by assuming that the standard specific volume of proteins is as great as 0.77 cm^3/g, calculations of the molecular mass gave a value of 74 ± 1 kDa, which is about three times the known molecular mass (24 kDa) of monomeric PhaP1$_{Reu}$. The distance distribution function is also shown in Fig. 6. It was observed that the maximum distance corresponds to a D value of 86 ± 3 Å, a value that, for the effect of the width of the hydration layer, is slightly greater than the side length of the triangle. Finally, we noticed that the

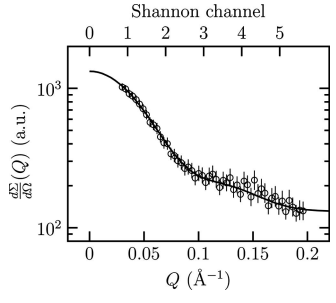

FIG. 5. Semilogarithmic SAXS profile of PhaP1. The line indicates the best fit obtained with the multipole expansion method. Q, scattering vector; a.u., arbitrary units.

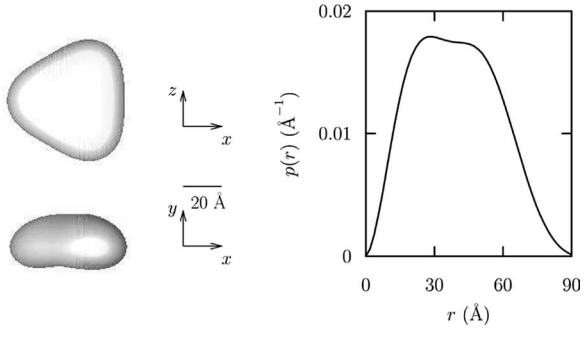

FIG. 6. Structure proposed for PhaP1. (Left panel) Shape reconstruction of PhaP1$_{Reu}$. (Right panel) Distance distribution function [$p(r)$] of PhaP1$_{Reu}$ calculated from the reconstructed shape.

number of Shannon channels, which are shown in Fig. 5, was greater than an *M* value of 5, confirming that the present analysis did not introduce an arbitrary high number of parameters.

DISCUSSION

The secondary structure predictions for the phasins sensu stricto showed comparable high proportions (about 90%) of α-helical structure. This structure could be a general characteristic of phasins. In this case the whole protein is a binding protein and probably has no additional function. The binding capacity is obviously not determined by a short motif conserved at the level of the primary structure but is probably due to the secondary structure and may also be due to the tertiary or quaternary structure of the protein.

The microscopic analyses and Western immunoblotting did not produce clear results. Both analyses indicated that there was binding of the PhaP1$_{Reu}$[ΔM]-EGFP, EGFP-PhaP1$_{Reu}$[N>112], and EGFP-PhaP1$_{Reu}$[ΔM] fusions. The PhaP1$_{Reu}$[113>C]-EGFP fusion did not bind to PHB granules in either experiment. The other fusions, such as PhaP1$_{Reu}$-[52-112]-EGFP, PhaP1$_{Reu}$[52>C]-EGFP, PhaP1$_{Reu}$[1-85]-EGFP, EGFP-PhaP1$_{Reu}$[N>85], and EGFP-PhaP1$_{Reu}$[52-112], gave no clear images or immunoblot results. Because of these binding characteristics, no region of PhaP1 that is obviously responsible for the binding of the fusions could be identified. None of the interesting regions, such as the N-terminal conserved part, the hydrophobic patch, or the alanine-rich C terminus, seem to represent PHB-binding domains, because all of the parts could be found in PHB-binding fusion proteins as well as in nonbinding fusion proteins (Fig. 3).

If the function of phasins is solely to stabilize the granules (i.e., dispersion of the hydrophobic PHB in the cytoplasm) and to prevent the coalescence of individual granules, like the coalescence that occurs in a *phaP1*$_{Reu}$ mutant (56, 40), it is likely that a certain structure of the whole protein is necessary and that no part can be eliminated without a loss of binding capacity. A high α-helix content throughout the whole protein could be a hint for similar structure and thus function of the complete protein. We found that the binding of the whole PhaP1$_{Reu}$ protein to PHB granules was better than the binding of any truncated PhaP1$_{Reu}$ protein. The SAXS analyses showed that PhaP1$_{Reu}$ does not bind to PHB as a monomer but binds as a homotrimer with a triangular and planar structure. This structure seems to be optimal to tightly cover the entire granule. This correlates very well with the results of Banki et al. (2), who showed that the stability of a phasin trimer bound to PHB granules was better than that of a PhaP1$_{Reu}$ monomer.

Very recently, the *Aeromonas hydrophila* phasin PhaP$_{Ahy}$ (13 kDa) was crystallized, and its structure was investigated by using X-ray analysis (59). The authors found a tetrameric structure for this phasin, which is not homologous to PhaP1$_{Reu}$ and therefore not a phasin sensu stricto. A tetramer of PhaP$_{Ahy}$ having a molecular mass of about 52 kDa is almost the same size as the PhaP1$_{Reu}$ trimer (60 kDa). A molecular mass of a PHB-binding unit of about 50 to 60 kDa is probably optimal to provide a layer at the surface of PHB granules.

From the revealed structure and size of the phasin protein, it was calculated that about 6,130 PhaP1$_{Reu}$ homotrimers or 18,390 individual PhaP1$_{Reu}$ molecules are necessary to completely cover the entire surface of a PHB granule with a diameter of 250 nm. Assuming that a single cell possesses about 20 such PHB granules in the late accumulation phase and that the average protein content of a single cell is about 0.155 pg (27), it can be calculated that PhaP1$_{Reu}$ accounts for about 7.8% of the total cellular protein. This is in good agreement with some previous estimates (50) and observations (56), although in other studies workers concluded that the phasin covers only 27 to 54% of the granule surface (52).

Surface coating of nanoparticles is an important part of nanoparticle synthesis. PHB granules are of interest especially for medical applications, as they are biodegradable and nontoxic. PHB forms water-insoluble intracellular inclusions (granules) that are accumulated as carbon and energy storage compounds in a large variety of prokaryotes. For optimized generation of functionalized nanoparticles based on phasin fusion proteins, knowledge about the binding of phasins to the granules should be helpful. It seems to be impossible to recognize a specific binding motif of phasins by in silico analyses. All four phasins of *R. eutropha* lack a highly conserved domain, but they have homologous hydrophobic regions. In addition, phasins occurring in other PHB-accumulating bacteria, like *Azotobacter vinelandii*, also do not have highly conserved amino acid residues.

ACKNOWLEDGMENTS

This study was supported in part by a grant provided by the Deutsche Forschungsgemeinschaft (grant Ste 386/6-4) and in part by the European Commission (contract 509012, NEST).

REFERENCES

1. **Anderson, A. J., and E. A. Dawes.** 1990. Occurrence, metabolism, metabolic role, and industrial uses of bacterial polyhydroxyalkanoates. Microbiol. Rev. **54:**450–472.
2. **Banki, M. R., T. U. Gerngross, and D. W. Wood.** 2005. Novel and economical purification of recombinant proteins: intein-mediated protein purification using in vivo polyhydroxybutyrate (PHB) matrix association. Protein Sci. **14:**1387–1395.
3. **Barnard, G. C., J. D. McCool, D. W. Wood, and T. U. Gerngross.** 2005. Integrated recombinant protein expression and purification platform based on *Ralstonia eutropha*. Appl. Environ. Microbiol. **71:**5735–5742.
4. **Bateman, A., L. Coin, R. Durbin, R. D. Finn, V. Hollich, S. Griffiths-Jones, A. Khanna, M. Marshall, S. Moxon, E. L. L. Sonnhammer, D. J. Studholme, C. Yeats, and S. R. Eddy.** 2004. The Pfam protein families database. Nucleic Acids Res. **32:**D138–D141.
5. **Birnboim, H. C., and J. Doly.** 1979. A rapid alkaline extraction procedure for screening recombinant plasmid DNA. Nucleic Acids Res. **7:**1513–1523.
6. **Deleage, G., C. Blanchet, and C. Geourjon.** 1997. Protein structure prediction. Implications for the biologist. Biochimie **79:**681–686.
7. **Friedrich, B., C. Hogrefe, and H. G. Schlegel.** 1981. Naturally occurring genetic transfer of hydrogen-oxidizing ability between strains of *Alcaligenes eutrophus*. J. Bacteriol. **147:**198–205.
8. **Griebel, R., Z. Smith, and J. M. Merrick.** 1968. Metabolism of poly-β-hydroxybutyrate. I. Purification composition and properties of native poly-β-hydroxybutyrate granules from *Bacillus megaterium.* Biochemistry **7:**3676–3681.
9. **Guermeur, Y., C. Geourjon, P. Gallinari, and G. Deleage.** 1999. Improved performance in protein secondary structure prediction by inhomogeneous score combination. Bioinformatics **15:**413–421.
10. **Guinier, A., and G. Fournet.** 1955. Small angle scattering of X-ray. Wiley, New York, NY.
11. **Hanahan, D.** 1983. Studies on transformation of *Escherichia coli* with plasmids. J. Mol. Biol. **166:**557–580.
12. **Hänisch, J., M. Wältermann, H. Robenek, and A. Steinbüchel.** 2006. The *Ralstonia eutropha* H16 phasin PhaP1 is targeted to intracellular triacylglycerol inclusions in *Rhodococcus opacus* PD630 and *Mycobacterium smegmatis* mc^{2}155 and provides an anchor to target other proteins. Microbiology **152:**3271–3280.
13. **Hänisch, J., M. Wältermann, H. Robenek, and A. Steinbüchel.** 2006. Eukaryotic lipid body proteins in oleogenous actinomycetes and their targeting

to intracellular triacylglycerol inclusions: impacts on model of lipid body biogenesis. Appl. Environ. Microbiol. **72:**6743–6750.
14. **Hoppert, M., and F. Mayer.** 1999. Principles of macromolecular organization and cell function in bacteria and archaea. Cell. Biochem. Biophysiol. **31:**247–284.
15. **Kataoka, M., Y. Hagihara, K. Mihara, and Y. Goto.** 1993. Molten globule of cytochrome c studied by the small angle X-ray scattering. J. Mol. Biol. **229:**591–596.
16. **Kataoka, M., I. Nishii, T. Fujisawa, T. Ueki, F. Tokunaga, and Y. Goto.** 1995. Structural characterization of molten globule and native states of apomyoglobin by solution X-ray scattering. J. Mol. Biol. **249:**215–228.
17. **King, R. D., and M. J. E. Sternberg.** 1996. Identification and application of the concepts important for accurate and reliable protein secondary structure prediction. Protein Sci. **5:**2298–2310.
18. **Koch, M., P. Vachette, and D. Svergun.** 2003. Small-angle scattering: a view on the properties, structures and structural changes of biological macromolecules in solution. Q. Rev. Biophys. **36:**147–227.
19. **Kovach, M. E, P. H. Elzer, D. S. Hill, G. T. Robertson, M. A. Farris, R. M. Roop, and K. M. Peterson.** 1995. Four new derivatives of the broad-host-range cloning vector pBBR1MCS, carrying different antibiotic-resistance cassettes. Gene **166:**175–176.
20. **Kyte, J., and R. F. Doolittle.** 1982. A simple method for displaying the hydropathic character of a protein. J. Mol. Biol. **157:**105–132.
21. **Laemmli, U. K.** 1970. Cleavage of structural proteins during the assembly of the head of bacteriophage T4. Nature **227:**680–685.
22. **Lee, S. J., J. P. Park, T. J. Park, S. Y. Lee, S. Lee, and J. K. Park.** 2005. Selective immobilization of fusion proteins on poly(hydroxyalkanoate) microbeads. Anal. Chem. **77:**5755–5759.
23. **Liebergesell, M., B. Schmidt, and A. Steinbüchel.** 1992. Isolation and identification of granule-associated proteins relevant for poly(3-hydroxybutyric acid) biosynthesis in *Chromatium vinosum* D. FEMS Microbiol. Lett. **99:**227–232.
24. **Maehara, A., S. Ueda, H. Nakano, and T. Yamane.** 1999. Analyses of a polyhydroxyalkanoic acid granule-associated 16 kilodalton protein and its putative regulator in the *pha* locus of *Paracoccus denitrificans*. J. Bacteriol. **181:**2914–2921.
25. **Marmur, J.** 1961. A procedure for the isolation of deoxyribonucleic acids from microorganisms. J. Mol. Biol. **3:**208–218.
26. **Moldes, C., P. Garcia, J. L. Garcia, and M. A. Prieto.** 2004. In vivo immobilization of fusion proteins on bioplastics by the novel tag BioF. Appl. Environ. Microbiol. **70:**3205–3212.
27. **Neidhardt, C., J. L. Ingraham, and M. Schaechter.** 1990. Physiology of the bacterial cell: a molecular approach. Sinauer Associates Inc., Sunderland, MA.
28. **Occhipinti, E., P. Martelli, F. Spinozzi, F. Corsi, C. Formantici, L. Molteni, H. Amenitsch, P. Mariani, P. Tortora, and R. Casadio.** 2003. 3D structure of *Sulfolobus solfataricus* carboxypeptidase developed by molecular modeling is confirmed by site-directed mutagenesis and small-angle X-ray scattering. Biophys. J. **85:**1165–1175.
29. **Ohura, T., K. I. Kasuya, and Y. Doi.** 1999. Cloning and characterization of the polyhydroxybutyrate depolymerase gene of *Pseudomonas stutzeri* and analysis of the function of substrate-binding domains. Appl. Environ. Microbiol. **65:**189–197.
30. **Park, T. J., J. P. Park, S. J. Lee, H. J. Hong, and S. Y. Lee.** 2006. Polyhydroxyalkanoate chip for the specific immobilization of recombinant proteins and its applications in immunodiagnostics. Biotechnol. Bioproc. Eng. **11:**173–177.
31. **Perez, J., P. Vachette, D. Russo, M. Desmadril, and D. Durand.** 2001. Heat-induced unfolding of neocarzinostatin, a small all-β protein investigated by small-angle X-ray scattering. J. Mol. Biol. **308:**721–743.
32. **Peters, V., and B. H. A. Rehm.** 2005. *In vivo* monitoring of PHA granule formation using GFP-labeled PHA synthase. FEMS Microbiol. Lett. **248:**93–100.
33. **Peters, V., and B. H. A. Rehm.** 2006. In vivo enzyme immobilization by use of engineered polyhydroxyalkanoate synthase. Appl. Environ. Microbiol. **72:**1777–1783.
34. **Pieper-Fürst, U., M. H. Madkour, F. Mayer, and A. Steinbüchel.** 1994. Purification and characterization of a 14-kDa protein that is bound to the surface of polyhydroxyalkanoic acid granules in *Rhodococcus ruber*. J. Bacteriol. **176:**4328–4337.
35. **Pieper-Fürst, U., M. H. Madkour, F. Mayer, and A. Steinbüchel.** 1995. Identification of the region of a 14-kDa protein of *Rhodococcus ruber* that is responsible for the binding of this phasin to polyhydroxyalkanoic acid granules. J. Bacteriol. **177:**2513–2523.
36. **Pohlmann, A., W. F. Fricke, F. Reinecke, B. Kusian, H. Liesegang, R. Cramm, T. Eitinger, C. Ewering, M. Pötter, E. Schwartz, A. Strittmatter, I. Voβ, G. Gottschalk, A. Steinbüchel, B. Friedrich, and B. Bowien.** 2006. Genome sequence of the bioplastic-producing "Knallgas" bacterium *Ralstonia eutropha* H16. Nat. Biotechnol. **24:**1257–1262.
37. **Pollack, L., M. W. Tate, N. C. Darnton, J. B. Knight, S. M. Gruner, W. A. Eaton, and R. H. Austin.** 1999. Compactness of the denatured state of a fast-folding protein measured by submillisecond small angle X-ray scattering. Proc. Natl. Acad. Sci. USA **96:**10115–10117.
38. **Pötter, M., M. H. Madkour, F. Mayer, and A. Steinbüchel.** 2002. Regulation of phasin expression and polyhydroxyalkanoate (PHA) granule formation in *Ralstonia eutropha* H16. Microbiology **148:**2413–2426.
39. **Pötter, M., H. Müller, F. Reinecke, R. Wieczorek, F. Fricke, B. Bowien, B. Friedrich, and A. Steinbüchel.** 2004. The complex structure of polyhydroxybutyrate (PHB) granules: four orthologous and paralogous phasins occur in *Ralstonia eutropha*. Microbiology **150:**2301–2311.
40. **Pötter, M., H. Müller, and A. Steinbüchel.** 2005. Influence of homologous phasins (PhaP) on PHA accumulation and regulation of their expression by the transcription repressor PhaR in *Ralstonia eutropha* H16. Microbiology **151:**825–833.
41. **Pötter, M., and A. Steinbüchel.** 2005. Poly(3-hydroxybutyrate) granule-associated proteins: impacts on poly(3-hydroxybutyrate) synthesis and degradation. Biomacromolecules **6:**552–560.
42. **Pötter, M., and A. Steinbüchel.** 2006. Biogenesis and structure of polyhydroxyalkanoate granules, p. 109–136. *In* J. M. Shively (ed.), Inclusions in prokaryotes. Microbiology monographs, vol. 1. Springer, Heidelberg, Germany.
43. **Rost, B., and C. Sander.** 1993. Prediction of protein secondary structure at better than 70 percent accuracy. J. Mol. Biol. **232:**584–599.
44. **Sambrook, J., E. F. Fritsch, and T. Maniatis.** 1989. Molecular cloning: a laboratory manual, 2nd ed. Cold Spring Harbor Laboratory, Cold Spring Harbor, NY.
45. **Schlegel, H. G., G. Gottschalk, and V. Bartha.** 1961. Formation and utilization of poly-β-hydroxybutyric acid by knallgas bacteria (*Hydrogenomonas*). Nature **29:**463–465.
46. **Schlegel, H. G., H. Kaltwasser, and G. Gottschalk.** 1961. Ein Submersverfahren zur Kultur wasserstoffoxidierender Bakterien: Wachstumsphysiologische Untersuchungen. Arch. Mikrobiol. **38:**209–222.
47. **Simon, R., U. Priefer, and A. Pühler.** 1983. A broad host range mobilization system for *in vivo* genetic engineering: transposon mutagenesis in Gram-negative bacteria. Bio/Technology **1:**784–791.
48. **Spinozzi, F., F. Carsughi, and P. Mariani.** 1998. Particle shape reconstruction by small-angle scattering: integration of group theory and maximum entropy to multipole expansion method. J. Chem. Phys. **109:**10148–10158.
49. **Steinbüchel, A., and H. G. Schlegel.** 1989. Excretion of pyruvate by mutants of *Alcaligenes eutrophus*, which are impaired in the accumulation of poly(β-hydroxybutyric acid) (PHB), under conditions permissive for synthesis of PHB. Appl. Microbiol. Biotechnol. **31:**168–175.
50. **Steinbüchel, A., K. Aerts, W. Babel, C. Föllner, M. Liebergesell, M. H. Madkour, F. Mayer, U. Pieper-Fürst, A. Pries, H. E. Valentin, and R. Wieczorek.** 1995. Considerations on the structure and biochemistry of bacterial polyhydroxyalkanoic acid inclusions. Can. J. Microbiol. **41**(Suppl. 1)**:**94–105.
51. **Tessmer, N., S. König, R. Reichelt, M. Pötter, and A. Steinbüchel.** 2007. Heat shock protein HspA and other proteins mimicking the function of phasins *sensu stricto* in recombinant strains of *Escherichia coli* accumulating polythioesters or polyhydroxyalkanoates. Microbiology **153:**366–374.
52. **Tian, J., A. He, A. G. Lawrence, P. Liu, N. Watson, A. J. Sinskey, and J. Stubbe.** 2005. Analysis of transient polyhydroxybutyrate production in *Wautersia eutropha* H16 by quantitative Western analysis and transmission electron microscopy. J. Bacteriol. **187:**3825–3832.
53. **Towbin, H., T. Staehelin, and J. Gordon.** 1979. Electrophoretic transfer of proteins from polyacrylamide gels to nitrocellulose sheets: procedure and some applications. Proc. Natl. Acad. Sci. USA **76:**4350–4354.
54. **Trewhella, J.** 1997. Insights into biomolecular function from small-angle scattering. Curr. Opin. Struct. Biol. **7:**702–708.
55. Reference deleted.
56. **Wieczorek, R., A. Pries, A. Steinbüchel, and F. Mayer.** 1995. Analysis of a 24-kDa protein associated with the polyhydroxyalkanoic acid granules in *Alcaligenes eutrophus*. J. Bacteriol. **177:**2425–2435.
57. **Williamson, D. H., and J. F. Wilkinson.** 1958. The isolation and estimation of the poly-β-hydroxybutyrate inclusions of *Bacillus* species. J. Gen. Microbiol. **19:**198–209.
58. **York, G. M., J. Stubbe, and A. J. Sinskey.** 2002. The *Ralstonia eutropha* PhaR protein couples synthesis of the PhaP phasin to the presence of polyhydroxybutyrate in cells and promotes polyhydroxybutyrate production. J. Bacteriol. **184:**59–66.
59. **Zhao, M., Z. Li, W. Zheng, Z. Lou, and G.-Q. Chen.** 2006. Crystallization and initial X-ray analysis of polyhydroxyalkanoate granule-associated protein from *Aeromonas hydrophila*. Acta Crystallogr. Sect. F **62:**814–819.